Flow interactions between uncoordinated flapping swimmers give rise to group cohesion

Joel W. Newbolt[a,b], Jun Zhang[a,b,c,1], and Leif Ristroph[a,1]

[a]Applied Math Lab, Courant Institute, New York University, New York, NY 10012; [b]Department of Physics, New York University, New York, NY 10003; and [c]New York University–East China Normal University (NYU-ECNU) Institute of Physics, NYU Shanghai, Shanghai 200062, China

Edited by Kenneth S. Breuer, Brown University, Providence, RI, and accepted by Editorial Board Member John D. Weeks December 19, 2018 (received for review September 17, 2018)

Many species of fish and birds travel in groups, yet the role of fluid-mediated interactions in schools and flocks is not fully understood. Previous fluid-dynamical models of these collective behaviors assume that all individuals flap identically, whereas animal groups involve variations across members as well as active modifications of wing or fin motions. To study the roles of flapping kinematics and flow interactions, we design a minimal robotic "school" of two hydrofoils swimming in tandem. The flapping kinematics of each foil are independently prescribed and systematically varied, while the forward swimming motions are free and result from the fluid forces. Surprisingly, a pair of uncoordinated foils with dissimilar kinematics can swim together cohesively—without separating or colliding—due to the interaction of the follower with the wake left by the leader. For equal flapping frequencies, the follower experiences stable positions in the leader's wake, with locations that can be controlled by flapping amplitude and phase. Further, a follower with lower flapping speed can defy expectation and keep up with the leader, whereas a faster-flapping follower can be buffered from collision and oscillate in the leader's wake. We formulate a reduced-order model which produces remarkable agreement with all experimentally observed modes by relating the follower's thrust to its flapping speed relative to the wake flow. These results show how flapping kinematics can be used to control locomotion within wakes, and that flow interactions provide a mechanism which promotes group cohesion.

collective locomotion | hydrodynamic interaction | flapping flight | fish schooling | bird flocking

When objects or organisms move within a fluid, they can interact via the flows they generate, as in the aerodynamic slipstreaming of cyclists or drafting of race cars. At large scales and high speeds (high Reynolds numbers), fluid inertia causes the motion of a body to leave behind a wake flow that develops in time as the wake exchanges momentum with the surrounding fluid and other bodies (1). The inertial fluid maintains a "memory" of past motions that is reflected in the interactions among bodies (2). The biological world provides many examples in which such interactions are seemingly exploited, such as tandem-wing flight of dragonflies (3, 4), collective wing fanning for beehive ventilation (5), and group locomotion of fish schools and bird flocks (6, 7).

It is a long-held hypothesis that swimming and flying animals come together to benefit from flow interactions. Seminal works include the calculations of Lissaman and Shollenberger (8) that show birds flying abreast or in a V-formation benefit from the upwash generated by the wingtip vortices of their neighbors, as well as the calculations of Weihs (9) that predict fish swimming in schools can find regions of reduced oncoming flow within the vortex arrays left by upstream neighbors. Sir James Lighthill (10) further suggested that the order in a school may come about passively from flow-mediated interactions among members. Yet the relatively few quantitative studies on animal groups leave the role of flows as an open question, and the prevailing models remain largely untested by physical experiments.

A proven strategy for studying the fluid dynamics of animal swimming or flight is to use actively flapping hydrofoils or airfoils as analogues of fins or wings (11–18). In particular, the forward flight of birds and steady swimming of fish have been studied experimentally and theoretically using actuated foils either fixed within an external flow or self-propelling through a fluid (13–18). Because this approach allows for precise control and measurement of motions, forces, and flows, it has helped reveal the fundamental mechanisms underlying flapping locomotion for foils operating in biologically relevant regimes of physical parameters. The primary signature of thrust production for fish and birds is a wake consisting of a staggered array of counterrotating vortices with a backward-directed jet-like average flow (19–22), a flow structure which has been reproduced and further studied using flapping foils (13, 23–26).

Recently, researchers have extended this strategy of using systems of flapping foils to study biologically inspired flow interactions (2, 18, 27–29). Progress has been made by studies focusing on the two-body problem using free-swimming foils in tandem that passively interact through the surrounding fluid (27, 28). When driven with identical flapping kinematics, the follower is seen to take up one of several discrete, stable positions within the wake of the leader, and the two travel together at the same speed. These results raise interesting questions about how passive flow interactions can help organize animal groups.

However, these recent results on flow-induced ordering would seem to be undermined if one relaxes the assumption that all

Significance

Fish and birds moving in groups are thought to benefit from hydrodynamic or aerodynamic interactions between individuals. To better understand these effects, we devise a robotic "school" of flapping swimmers whose formations and motions come about from flow interactions. Surprisingly, we find that the flows naturally generated during swimming can also prevent collisions and separations, allowing even uncoordinated individuals with different flapping motions to travel together. Other benefits include freeloading by a "lazy" follower who keeps up with a faster-flapping leader by surfing on its wake. More generally, our study provides complete maps linking flapping motions to group locomotion, which is needed to test whether flow interactions are also exploited by animals.

Author contributions: J.W.N., J.Z., and L.R. designed research; J.W.N. performed research; J.W.N., J.Z., and L.R. analyzed data; and J.W.N., J.Z., and L.R. wrote the paper.

The authors declare no conflict of interest.

This article is a PNAS Direct Submission. K.S.B. is a guest editor invited by the Editorial Board.

[1]To whom correspondence may be addressed. Email: ristroph@cims.nyu.edu or jun@cims.nyu.edu.

This article contains supporting information online at www.pnas.org/lookup/suppl/doi:10.1073/pnas.1816098116/-/DCSupplemental.

Published online January 30, 2019.

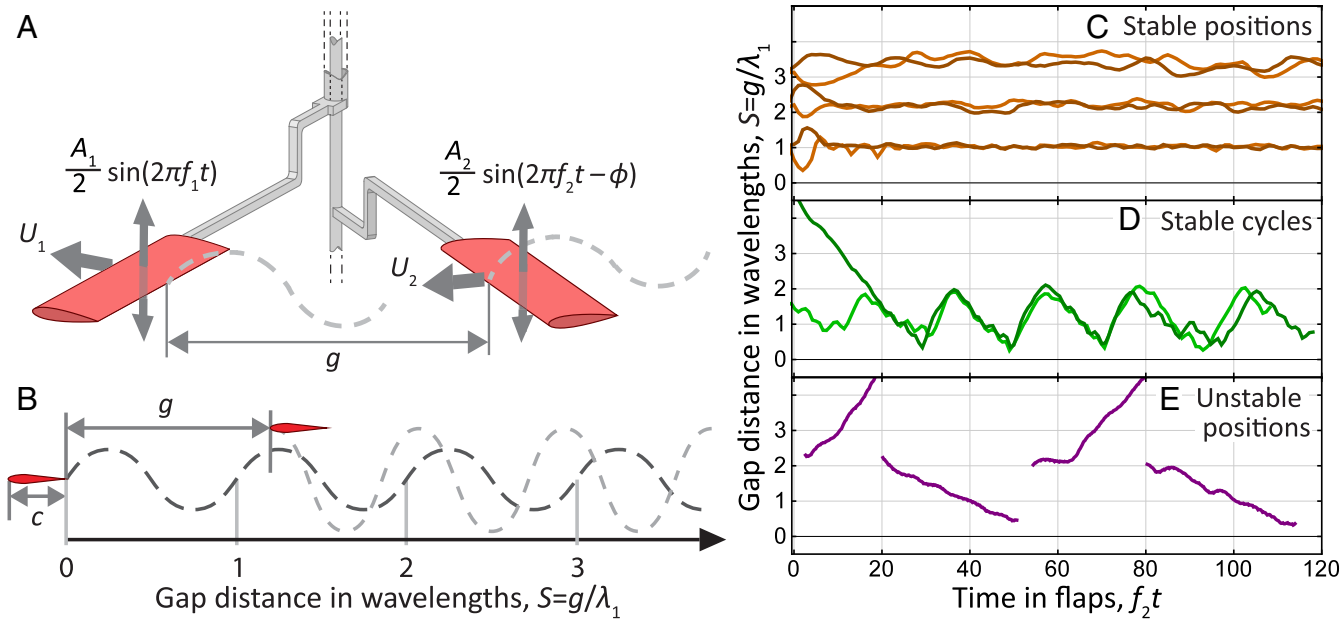

Fig. 1. (*A*) Two tandem hydrofoils are flapped independently by separate motors mounted above a water tank (motors and tank not shown; full photo in *SI Appendix*, Fig. S1). Each axle is flapped up and down, but is free to rotate, causing the foils to swim independently in a large, horizontal circle. (*B*) A dimensionless gap distance is measured in terms of the leader's wavelength, $S \equiv g/\lambda_1$. (*C*–*E*) For a given amplitude and frequency, the leader swims at constant speed (averaged over one flap) while the follower has multiple distinct states, including (*C*) multiple stable positions for $f_2/f_1 = 1$, $A_2/A_1 = 1$, and $\phi = 0$, (*D*) stable cycles for $f_2/f_1 < 1$ and $A_2 f_2/A_1 f_1 > 1$, and (*E*) unstable positions for $f_2/f_1 > 1$ and $A_2 f_2/A_1 f_1 < 1$. Each plot shows separate lines for experimental trials with different initial conditions.

locomotors have identical flapping motions. Animal groups, after all, are composed of independent individuals whose kinematics vary. In fact, it has been observed that fish in the back of a school tend to swim with lower tail-beat frequency (30) and birds flying in formation do not synchronize the motion of their wings (31). Here we ask whether coherent collective locomotion may arise from the interactions among uncoordinated individuals. Understanding the effects of changing an individual's flapping kinematics is fundamental to understanding group dynamics, because real fish and birds use active feedback to control their speed and position through changes in their flapping kinematics. We study this problem in the simple setting of two tandem foils driven with dissimilar flapping kinematics and whose motions and spacing are dynamically determined through flow interactions. We identify surprisingly broad ranges in the parameter space of kinematics for which the pair "schools" together, including modes in which an underdriven follower may "freeload" and keep up with the leader by exploiting its flows.

Experimental Methods and Observed States

Our experiment consists of two hydrofoils supported on two concentric vertical axles and immersed in a water tank, as shown in Fig. 1*A* and detailed in *SI Appendix*. Vertical oscillations, or flapping motions, are imparted to the foils using two independent motors that connect to the axles via rotary bearings, permitting free revolution of each foil about its axle (2, 13, 27). Horizontal locomotion arises from the fluid forces acting on the foils and takes the form of rotational orbits about the tank. Importantly, this system permits distinct flapping motions for the leader #1 and follower #2 foils, $y_1 = (1/2)A_1 \sin(2\pi f_1 t)$ and $y_2 = (1/2)A_2 \sin(2\pi f_2 t - \phi)$, and we explore ranges for the peak-to-peak amplitudes $A_{1,2} = 0$ to 4 cm, frequencies $f_{1,2} = 0$ to 4 Hz, and initial phases $\phi \in [0, 2\pi)$. Fixed geometric parameters include chord length $c = 4$ cm, span length 15 cm, and radial distance from rotation axis to foil midspan 32 cm. An optical encoder on each axle records the rotational motion, from which the translational speeds $U_{1,2} = 18$ to 28 cm/s (at midspan) and leader–follower gap distance g are computed. The resulting Reynolds numbers $\mathrm{Re} = cU/\nu \approx 10^3$ to 10^4 and Strouhal numbers $\mathrm{St} = Af/U = 0.21$ to 0.23 are relevant to fish swimming and bird flight (14, 24), where ν is the kinematic viscosity of the fluid. The dimensionless kinematic parameters to be varied are the follower phase lag ϕ and the amplitude A_2/A_1 and frequency f_2/f_1 ratios.

When the foils are actuated and released, we observe that the leader achieves a period-averaged swimming speed U_1 that is nearly constant (within 4%). The leader's speed depends on its own kinematics but not on the motions of the follower. Thus, the dynamical states of the pair are characterized by the follower's motion relative to the leader, which may be quantified by the dimensionless separation $S \equiv g/\lambda_1$, where $\lambda_1 = U_1/f_1$ is the wavelength of the leader's swimming trajectory (Fig. 1*B*). In Fig. 1 *C*–*E*, we survey some of the observed states that are achieved by varying the foil kinematics (see also Movies S1–S3). For example, when $\phi = 0$, $A_2/A_1 = 1$, and $f_2/f_1 = 1$, the flapping motions are identical and the follower takes up one of several discrete stable positions behind the leader, and the two form a school that travels together. This mode corresponds well with previous studies (27, 28), and the preferred positions have nearly integer values of S. When the follower is overdriven, i.e., $A_2 f_2/A_1 f_1 > 1$, and $f_2/f_1 < 1$, the initial phase ϕ is unimportant, since the phase changes continuously, and the follower alternates between fast and slow swimming, yielding what seem to be stable cycles of S. When the follower is underdriven, i.e., $A_2 f_2/A_1 f_1 < 1$, and $f_2/f_1 > 1$, we observe unstable positions for the follower, which either collides into or separates away from the leader, depending on the initial value of S and the initial difference in swimming speeds. The details of the modes, such as the threshold value of S for collision or separation, depend on the kinematic parameters.

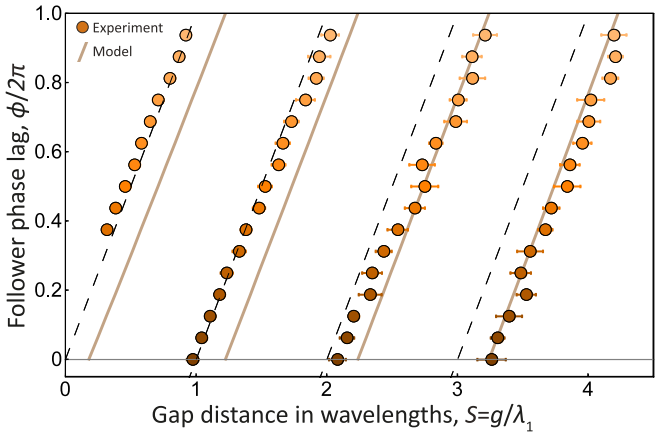

Fig. 2. Stable positions for the follower for varying phase difference ϕ at equal amplitude and frequency in experiment (circles) and model (brown lines). Increasing ϕ moves the stable positions downstream at a rate of roughly one wavelength per phase lag revolution, shown by the dashed lines $S=\phi/2\pi+\mathbb{Z}$. If the follower is forced from one of the stable positions, it can fall into an adjacent stable position roughly one wavelength away.

Varying Flapping Kinematics. We next investigate the origin of the different follower modes by systematically sweeping through the kinematic parameters. If $A_2/A_1=1$ and $f_2/f_1=1$ and only the phase lag ϕ is varied, we observe that the follower assumes one of several discrete positions behind the leader, and the pair travels together. Systematically varying ϕ and measuring all such stable positions yields the data points of Fig. 2. For the axis $\phi=0$, we recover the results of previous studies that the follower sits near integer values of S (27, 28). Increasing ϕ yields positions that are displaced downstream at approximately a rate of one wavelength per phase lag revolution, $\partial S/\partial(\phi/2\pi)\approx 1$. These stable positions are found only for $S\lesssim 4$, beyond which the foils do not maintain discrete separations, suggesting that the hydrodynamic interactions weaken with distance.

If $f_2/f_1=1$ is fixed and both ϕ and the amplitude ratio A_2/A_1 are varied, we discover a broad range in these parameters for which the follower stably positions behind the leader. In Fig. 3, we display all such states as circles and indicate their resulting separation distances S. In the stable region, the line $A_2/A_1=1$ repeats the results of Fig. 2, where increasing ϕ yields positions of larger S. When $A_2/A_1\neq 1$, increasing ϕ has this same effect, but the stable states are observed for a shorter range of S. Fixing ϕ and increasing A_2/A_1 beyond unity yields smaller S and thus a more compact pair that travels together, while decreasing A_2/A_1 below unity leads to a more dilated pair. These results show that, with the appropriate phase, the follower may keep up even when driven with as small as one-third of the amplitude of the leader. In other words, this freeloading follower swims at about 3 times the speed it would in isolation for the same flapping kinematics.

Above the stable region of Fig. 3, no stable positioning is observed, but rather an overdriven follower (i.e., $A_2/A_1>1$ when $f_2/f_1=1$) with an initial separation in the red region moves toward the leader, and S decreases. Such a follower may become caught in a stable position closer to the leader where the hydrodynamic interaction is stronger, or its inertia may carry it through these stable positions and cause a rear-end collision. Below the stable region, an underdriven follower ($A_2/A_1<1$) with an initial separation in the blue region moves away from the leader, and S increases. The separation then grows continuously, since the underdriven follower has a lower isolated swimming speed than the leader.

Finally, we remove our constraint on f_2/f_1, allowing the foils to have different flapping amplitudes and frequencies. We arrive at new, dynamic behaviors of the pair that are categorized in Fig. 4 across the kinematic parameter space of f_2/f_1 and A_2/A_1. In this case, the curve given by $A_1f_1=A_2f_2$ is an important boundary representing equal flapping speeds for the two foils and thus approximately equal swimming speeds, were they in isolation. The region above this curve represents conditions for an overdriven follower, and one expects collisions, but this is not always so. Likewise, the region below this curve corresponds to an underdriven follower, and one expects separation of the pair, but this is not always so. One violation of this expectation is the case of $f_2/f_1=1$, where we recover the stable position states for a range of A_2/A_1 near unity (Fig. 3). Two new behaviors are also observed. For $f_2/f_1<1$ but $A_2f_2/A_1f_1>1$ (green region), we achieve the stable-cycle mode introduced in Fig. 1*D*: The follower, despite being overdriven, does not collide with (or catch up to) the leader. For $f_2/f_1>1$ but $A_2f_2/A_1f_1<1$ (purple region), we achieve the unstable-position mode introduced in Fig. 1*E*, and the underdriven follower may collide with (or catch) the leader if the initial gap and speed difference is sufficiently small.

Follower-Wake Interaction Model. To interpret these findings, we formulate a minimal, reduced-order model that incorporates the interaction of the follower with the wake of the leader. Solutions to this model are displayed in Figs. 2–4 and show excellent agreement with our experiments. The model assumes that the thrust on each foil scales with the square of that foil's flapping speed relative to the ambient fluid, and the drag depends on the square of that foil's swimming speed (24, 32, 33). For the leader, which swims into quiescent fluid and thus moves as an isolated foil, the thrust is proportional to ${\dot{y}_1}^2\propto(A_1f_1)^2$ and drag to U_1^2, and the terminal swimming speed arises from a balance of these forces. Importantly, the thrust on the follower depends not only on its flapping speed $\dot{y}_2\propto A_2f_2$ but also on the vertical speed v of the leader's wake flow at the follower's location. We construct this wake by assuming that the leader leaves behind a wake flow that is equal to its flapping speed $v=\dot{y}_1$ as it swims through a specific

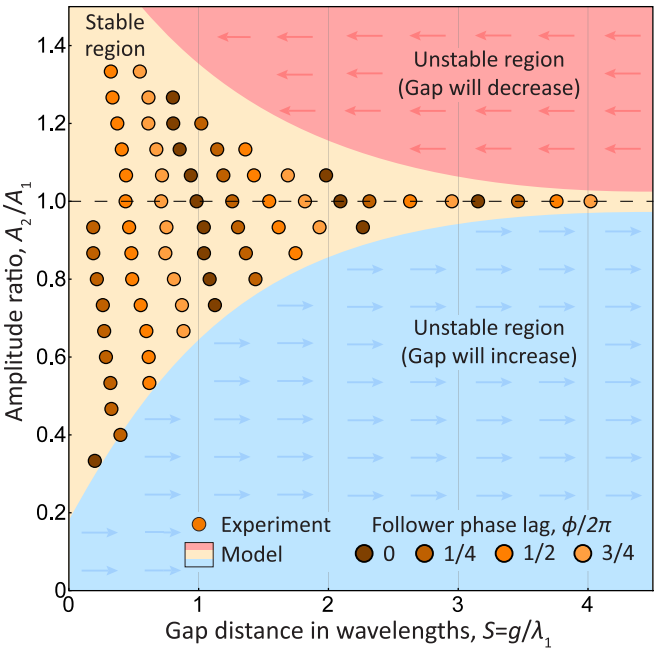

Fig. 3. Stable positions for the follower for varying amplitude ratio A_2/A_1 and phase difference ϕ at equal frequency in experiment (circles) and model (background color). At fixed ϕ, increasing A_2/A_1 compresses the pair, while decreasing A_2/A_1 leads to an increase in S, up to some threshold.

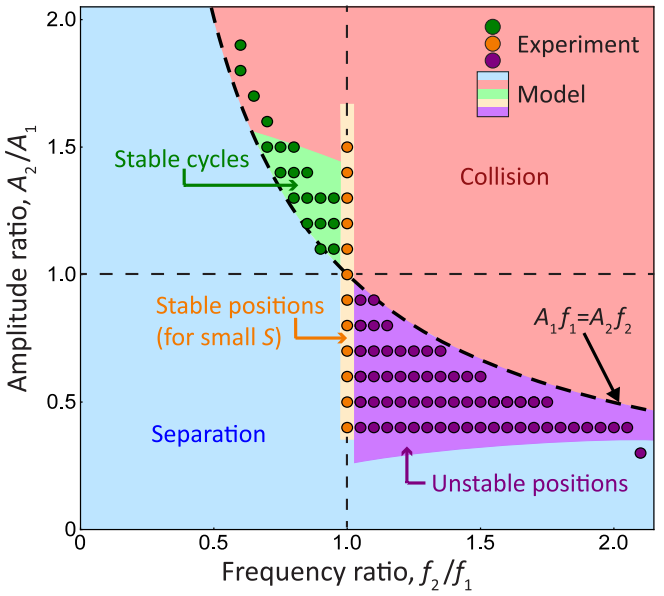

Fig. 4. Parameter space for two independently swimming hydrofoils. The dynamical state of the follower is categorized by color (Fig. 1 *C*–*E*) from experiment (circles) and model (background colors). The states with stable positions at $f_2/f_1 = 1$ (Fig. 3) divide regions where the follower has cyclic trajectories, $f_2/f_1 < 1$, and unstable trajectories, $f_2/f_1 > 1$.

position in the fluid. Thereafter, v decays exponentially with time constant τ, which (crudely) accounts for the dissipation of the coherent wake structure. Thus, the wake speed oscillates and decays with downstream distance, and it is this wave with which the follower interacts.

Based on this model, the follower dynamics are described by a delay differential equation that includes a period-averaged thrust that is proportional to

$$(\dot{y}_2 - v)^2 \propto (A_2 f_2)^2 + (A_1 f_1 e^{-\Delta t/\tau})^2 - 2A_1 f_1 A_2 f_2 e^{-\Delta t/\tau} \cos[(2\pi f_2 t - \phi) - 2\pi f_1 (t - \Delta t)].$$

Here Δt, which itself may vary in time, is the elapsed time since the leader passed through the follower's current position. This quantity captures the memory or history dependence of the interactions. The first term in the above expression is the bare thrust that the follower would have in isolation, and the second and third terms result from wake interactions.

The model provides hydrodynamic interpretations of the modes observed in our experiment. First, consider the case of identical, synchronized swimmers ($\phi = 0$, $A_2/A_1 = 1$, and $f_2/f_1 = 1$), for which the follower is observed to take up one of several locations downstream of the leader (data points from Fig. 2). The model (brown curve) identifies similar locations as stable equilibrium positions. Namely, the follower experiences higher thrust in portions of its stroke when it flaps counter to the wake flow but lower thrust in other portions as it flaps with the flow, and the identified stable positions are those for which the net or stroke-averaged thrust is unchanged relative to isolated swimming. The stability of these states is explained by considering positional perturbations. For example, at the middle of the upstroke, the follower has a stronger upward flow just ahead, and a forward perturbation is thus countered by lower thrust. Elaborations of this argument show that restoring forces come about from wake-induced modifications of thrust, and the multiplicity of stable states is related to the spatial periodicity of the wake flow.

For asynchronous swimmers ($\phi \neq 0$), the same follower-wake stabilization is achieved at an appropriately shifted position. The extent to which the follower flaps with or against the wake flow is determined by the phase difference between the follower's wavy trajectory and the wave-like wake of the leader. Using the model's assumptions about the wake structure, we can quantify the phase difference between the wake flow and the follower's flapping as $\phi_S/2\pi = \phi/2\pi - S$. A fixed value of ϕ_S ensures that the thrust the follower experiences within the wake flow is maintained. Thus, ϕ and S must increase together for the pair to swim at the same speed, explaining the trends of Fig. 2.

If the follower's amplitude is changed such that $A_2/A_1 \neq 1$, a new position is taken up and stabilized by the same mechanism. As shown in the stable (tan colored) region of Fig. 3, increasing A_2 for fixed ϕ leads to smaller S. This is explained by the increase in the "bare" thrust associated with faster flapping but a compensating decrease in thrust associated with moving closer to the leader, where the follower's upstroke occurs in a stronger upward flow. For larger S, the decay of the wake flow leads to a diminished range of A_2/A_1 that can be stabilized.

The stable cycles (green region) and unstable positions (purple) of Fig. 4 for $f_2/f_1 \neq 1$ are more complex. Some intuition can be gained by considering the mismatched frequencies as a continuous drift of temporal phase $\phi \propto (f_1 - f_2)t$ and by viewing the wake interactions as tending to drive the follower toward a preferred value of $\phi_S/2\pi = \phi/2\pi - S$. Drifting of ϕ must be accompanied by changing S, explaining why only dynamic modes appear under these conditions. Further interpretations of all states can be found in *SI Appendix*.

Discussion

Our results reveal the locomotion dynamics of actively flapping and passively interacting foils. Within the two-body problem, our experiments and model show that purely hydrodynamic interactions lead to surprisingly "life-like" collective dynamics. One example is the stable-position mode, in which a follower falls into specific positions behind the leader due to wake interactions, and the pair travels together. This well-ordered "schooling" occurs even for asynchronous individuals with dissimilar flapping phases, and also for individuals with dissimilar amplitudes and thus different isolated swimming speeds. Flow interactions provide a robust mechanism for maintaining group cohesion by allowing weakly flapping, or "lazy," followers to keep up with a leader, and also preventing rear-end collisions of faster-flapping followers. Cohesion is also preserved for dissimilar flapping frequencies in the stable-cycle mode, in which a faster-flapping follower undergoes bouts of gaining on a leader only to then be carried downstream by the wake. More generally, our study furnishes complete maps of the degree of kinematic dissimilarity that leads to cohesive modes versus collision of members or their separation and fracturing of the group.

An alternative interpretation of our results is that they reveal how active changes in flapping kinematics can be used to control locomotion within a group and within the associated wake flows. Our work shows that these hydrodynamic interactions can be potentially advantageous. For example, to keep pace with a faster-flapping leader, a lazy follower can flap with significantly lower amplitude and exploit the stable-position mode. To reach any desired position behind a leader, a follower should simply modify its flapping phase. To successfully pursue and catch up to a fast-flapping leader, a follower should use high-frequency, low-amplitude motions to exploit the unstable-position mode. To successfully evade a faster-flapping follower, a leader should use high-frequency, low-amplitude motions to exploit the stable-cycle mode. Generally, our maps outline the kinematic strategies available to interacting locomotors.

Our study reveals a broad range of parameters for which flapping foils school together even with uncoordinated kinematics and a lack of active feedback. The observed modes stem from the coherent interactions between an oscillating body with the

wave-like flow generated by an upstream neighbor, a feature that has been observed in experiments on fish swimming in vortex-laden flows (34, 35) and in recent studies of the motions of birds in formation flight (31). Our results provide a baseline of passive dynamics to compare with the active dynamics of real animal groups, wherein each member can also use active feedback. Prior experiments on fish swimming in a wake flow show evidence that their active behavior is indeed related to their passive dynamics (35).

Our results on lazy followers build on a growing body of literature that shows undulatory swimmers can take advantage of the flows present in wakes. One line of research has investigated swimmers in the drag wake produced by a stationary obstacle, where the fluid in the wake moves at a lower speed than the oncoming flow, and, close behind the obstacle, the flow even reverses direction. Experiments have shown that fish swimming in such a wake have decreased muscle activity (34), and related models indicate an increase in swimming efficiency (36). Experiments and simulations have also shown that even completely inactive "swimmers" (i.e., passive and undriven) may be pulled upstream due to interactions with a drag wake (35, 37). More relevant to group locomotion is the case of swimming within a thrust wake, like that generated by an upstream swimmer. Simulations have shown that a completely inactive body can also be pulled upstream in a thrust wake (38), and models have also shown increased efficiency for active swimming in thrust wakes (36). This is perhaps more surprising than the results in drag wakes, because a swimmer within a thrust wake experiences an oncoming flow that is faster than it would encounter outside the wake. Our experiments reveal that a weakly flapping follower can swim at much faster speeds when swimming in the thrust wake created by an upstream neighbor, and that this benefit arises spontaneously due to passive repositioning within the wake flow. Further, our model attributes this increased speed to the increased thrust produced when the follower flaps against transverse flows, a feature that is present in both thrust and drag wakes.

Our results also show how collective locomotion depends on the combined effects of flapping kinematics and wake-flow interactions, which is relevant to schools of fish whose members have different tail-beat frequencies (30) as well as the formation flight of birds with asynchronous flapping (31). Our model verifies that an individual's dynamics depend on the phase difference between its flapping motion and the wake flow it encounters, a quantity that is also important in the tandem-wing flight of dragonflies (3, 4) and the flow enhancement generated by tandem bees flapping their wings for hive ventilation (5). Problems concerning flow-mediated interactions in general may benefit from the framework of our model and its simple assumption that forces are modified according to relative flows.

Materials and Methods

Experimental Apparatus. The experimental apparatus is constructed to heave two hydrofoils up and down while allowing them to swim freely and independently in circular paths in a horizontal plane (*SI Appendix*, Fig. S1). The foils are NACA0017, made with 3D-printed polylactic acid (PLA), with chord $c = 4$ cm, span $s = 15$ cm, and distance from rotation axis to foil midspan $R = 31.7$ cm; they swim in a cylindrical water tank of diameter 92 cm and water depth 58 cm and have a midflap height at 17 cm below a solid, acrylic top.

The foils are kept independent by having two concentric vertical axles; the outer axle is hollow with the inner axle passing through. Each axle is oscillated vertically by a separate motor and held by rotational bearings allowing them to rotate with negligible resistance. For large values of R/c, the rotational motion approximates free translational motion (here $R/c = 7.9$). The vertical flapping of the foils is driven via Scotch yokes which convert the rotations of the two stepper motors to sinusoidal vertical oscillations of the axles. The flapping amplitude is set by an adjustable-offset eccentric shaft attached to the motor shaft, while the frequency and phase of the motors are controlled by an Arduino computer. The displacement in the swimming direction of each foil is measured by rotary optical encoders mounted on each axle, and the data are logged to a computer for later analysis. Because both g and λ_1 increase linearly with distance from the axis of rotation, the dimensionless separation S depends only weakly on the radial distance at which it is measured.

Opposite each foil is a counterweight and a drag load, which consists of a cylinder, mesh, and a frame (see *SI Appendix*, Fig. S1C). The counterweight serves to improve the performance of the axle bearings, while the purpose of the drag load is to reduce the free swimming speed of each foil to increase the Strouhal number into the range known for maximum efficiency and most commonly seen in biological locomotion (24) (here $\mathrm{St} = Af/U = 0.21$ to 0.23).

Follower-Wake Interaction Model. The follower dynamics described by *SI Appendix*, Eq. **S7** are numerically integrated in Mathematica using an Euler method with a time step $\leq 1/250$ of a flapping period. The initial swimming speed of each foil is set to the steady swimming speed of the leader and the initial separation is systematically varied. A conditional statement excludes the wake interaction before the follower overtakes the leader's starting position, and another statement catches collisions and terminates the integration. If run sufficiently long, the system exhibits states that may be classified according to the leader–follower gap distance $g = x_1 - x_2$ at long times. Constant $g > 0$ implies stable positioning of the follower, time-varying but bounded $g > 0$ implies stable cycling, $g = 0$ at some time implies collision, and $\dot{g} > 0$ implies separation. If the terminal conditions $g = 0$ or $\dot{g} > 0$ are achieved with different initial conditions, then the state is termed unstable positioning.

For the reported model results, we have used parameter values estimated from the experiments and summarized in *SI Appendix*, Table S1. The fluid density ρ, wing chord length c, and span length s are measured directly. Mapping our rotational experiments to a translational model requires conversion of torques to effective forces and moment of inertia to an effective mass. This mapping necessitates the choice of a radial distance at which forces can be viewed as acting, and we opt for the distance from the central axle to the midspan of the wings, $R = 31.7$ cm. This choice matches the center-of-thrust location expected for a uniform thrust distribution along the span. The effective mass is then given by $m = I/R^2$, where the moment of inertia I is calculated using the measured masses and geometry of the wing, support arm, central axle, etc., as well as the parallel axis theorem. A calculation of the added mass of the surrounding fluid shows that it is significantly less than the effective solid mass, and so we neglect this effect.

For the thrust coefficient $C_T = 4\langle F_T \rangle / \rho c s (\pi A f)^2$, previous measurements (24, 33) indicate $C_T \approx 0.8$ to 1.1, after conversion to our nondimensionalization in terms of the flapping speed. The specific value of $C_T = 0.96$ is selected by comparing model results to the experimental data of Figs. 3 and 4, and varying this value yields the same states but with somewhat different boundaries. The drag coefficient C_D is then estimated by noting the nearly constant $\mathrm{St} = 0.23$ for isolated foils observed in experiments and using the relation $C_D = \pi^2 C_T \mathrm{St}^2/2$. The wake decay time constant τ is estimated based on comparison with the experimental data of Fig. 3. The specific value of $\tau = 0.5$ s is similar to that inferred in our previous studies on similar experimental systems (2, 27).

Further details of the experimental apparatus and follower-wake interaction model, as well as further interpretation of the results and movies, can be found in *SI Appendix*.

ACKNOWLEDGMENTS. For their helpful discussions, we thank Sophie Ramananarivo, Anand Oza, Stephen Childress, Michael Shelley, and Eva Kanso. We acknowledge funding provided by New York University (NYU) Graduate School of Arts and Science and NYU Global Seed.

1. Tritton DJ (1988) *Physical Fluid Dynamics* (Clarendon Press, Oxford).
2. Becker AD, Masoud H, Newbolt JW, Shelley M, Ristroph L (2015) Hydrodynamic schooling of flapping swimmers. *Nat Commun* 6:8514.
3. Wang ZJ, Russell D (2007) Effect of forewing and hindwing interactions on aerodynamic forces and power in hovering dragonfly flight. *Phys Rev Lett* 99: 148101.
4. Lehmann F-O (2009) Wing–wake interaction reduces power consumption in insect tandem wings. *Exp Fluids* 46:765–775.
5. Gravish N, Peters JM, Combes SA, Wood RJ (2015) Collective flow enhancement by tandem flapping wings. *Phys Rev Lett* 115:188101.
6. Partridge BL (1982) Structure and function of fish schools. *Sci Am* 246:114–123.
7. Bajec IL, Heppner FH (2009) Organized flight in birds. *Anim Behav* 78:777–789.

8. Lissaman PBS, Shollenberger CA (1970) Formation flight of birds. *Science* 168:1003–1005.
9. Weihs D (1973) Hydromechanics of fish schooling. *Nature* 241:290–291.
10. Lighthill J (1975) *Mathematical Biofluiddynamics* (Society for Industrial and Applied Mathematics, Philadelphia).
11. Ellington CP, Van Den Berg C, Willmott AP, Thomas ALR (1996) Leading-edge vortices in insect flight. *Nature* 384:626–630.
12. Dickinson MH, Lehmann F-O, Sane SP (1999) Wing rotation and the aerodynamic basis of insect flight. *Science* 284:1954–1960.
13. Vandenberghe N, Zhang J, Childress S (2004) Symmetry breaking leads to forward flapping flight. *J Fluid Mech* 506:147–155.
14. Taylor GK, Nudds RL, Thomas ALR (2003) Flying and swimming animals cruise at a strouhal number tuned for high power efficiency. *Nature* 425:707–711.
15. Triantafyllou MS, Techet AH, Hover FS (2004) Review of experimental work in biomimetic foils. *IEEE J Oceanic Eng* 29:585–594.
16. Lauder GV, et al. (2011) Robotic models for studying undulatory locomotion in fishes. *Mar Technol Soc J* 45:41–55.
17. Taylor G, Triantafyllou MS, Cameron T (2010) *Animal Locomotion* (Springer, New York).
18. Platzer MF, Jones KD, Young J, Lai JCS (2008) Flapping wing aerodynamics: Progress and challenges. *AIAA J* 46:2136–2149.
19. Blickhan R, Krick C, Zehren D, Nachtigall W, Breithaupt T (1992) Generation of a vortex chain in the wake of a suhundulatory swimmer. *Naturwissenschaften* 79:220–221.
20. Müller UK, Van Den Heuvel BLE, Stamhuis EJ, Videler JJ (1997) Fish foot prints: Morphology and energetics of the wake behind a continuously swimming mullet (chelon labrosus risso). *J Exp Biol* 200:2893–2906.
21. Kokshaysky NV (1979) Tracing the wake of a flying bird. *Nature* 279:146–148.
22. Spedding GR (1987) The wake of a kestrel (*Falco tinnunculus*) in flapping flight. *J Exp Biol* 127:59–78.
23. Lighthill J (1969) Hydromechanics of aquatic animal propulsion. *Annu Rev Fluid Mech* 1:413–446.
24. Triantafyllou GS, Triantafyllou MS, Grosenbaugh MA (1993) Optimal thrust development in oscillating foils with application to fish propulsion. *J Fluids Struct* 7: 205–224.
25. Streitlien K, Triantafyllou GS, Triantafyllou MS (1996) Efficient foil propulsion through vortex control. *AIAA J* 34:2315–2319.
26. Andersen A, Bohr T, Schnipper T, Walther JH (2017) Wake structure and thrust generation of a flapping foil in two-dimensional flow. *J Fluid Mech* 812:R4.
27. Ramananarivo S, Fang F, Oza A, Zhang J, Ristroph L (2016) Flow interactions lead to orderly formations of flapping wings in forward flight. *Phys Rev Fluids* 1: 071201.
28. Zhu X, He G, Zhang X (2014) Flow-mediated interactions between two self-propelled flapping filaments in tandem configuration. *Phys Rev Lett* 113:238105.
29. Im S, Park SG, Cho Y, Sung HJ (2018) Schooling behavior of rigid and flexible heaving airfoils. *Int J Heat Fluid Flow* 69:224–233.
30. Svendsen JC, Skov J, Bildsoe M, Steffensen JF (2003) Intra-school positional preference and reduced tail beat frequency in trailing positions in schooling roach under experimental conditions. *J Fish Biol* 62:834–846.
31. Portugal SJ, et al. (2014) Upwash exploitation and downwash avoidance by flap phasing in ibis formation flight. *Nature* 505:399–402.
32. Wu TY (1961) Swimming of a waving plate. *J Fluid Mech* 10:321–344.
33. Floryan D, Van Buren T, Rowley CW, Smits AJ (2017) Scaling the propulsive performance of heaving and pitching foils. *J Fluid Mech* 822:386–397.
34. Liao JC, Beal DN, Lauder GV, Triantafyllou MS (2003) Fish exploiting vortices decrease muscle activity. *Science* 302:1566–1569.
35. Beal DN, Hover FS, Triantafyllou MS, Liao JC, Lauder GV (2006) Passive propulsion in vortex wakes. *J Fluid Mech* 549:385–402.
36. Alben S (2009) On the swimming of a flexible body in a vortex street. *J Fluid Mech* 635:27–45.
37. Eldredge JD, David P (2008) Passive locomotion of a simple articulated fish-like system in the wake of an obstacle. *J Fluid Mech* 607:279–288.
38. Oskouei BD, Kanso E (2013) Stability of passive locomotion in inviscid wakes. *Phys Fluids* 25:021901.